Frequency-Tunable High-Power Terahertz Wave Generation from GaP

doi: 10.1063/1.1560573

Frequency-tunable high-power terahertz wave generation from GaP

T. Tanabe[a] and K. Suto
Department of Materials Science, Graduate School of Engineering, Tohoku University, Aoba-yama 02, Sendai 980-8579, Japan

J. Nishizawa and T. Kimura
Semiconductor Research Institute, Kawauchi, Aoba-ku, Sendai 980-0862, Japan

K. Saito
Department of Materials Science, Graduate School of Engineering, Tohoku University, Aoba-yama 02, Sendai 980-8579, Japan

(Received 16 August 2002; accepted 22 January 2003)

A frequency-tunable terahertz wave was generated from GaP crystals using an optical parametric oscillator as the pump source and a YAG laser (1.064 μm) as the signal source. By tuning the very small angle, θ_{in}, between the pump and signal light beam directions, tunable terahertz waves over the frequency range from 0.5 to 3 THz were obtained. The THz frequency changed almost linearly with the angle θ_{in}. The precise noncollinear phase matching condition is discussed. The pulsed peak power of the THz wave was as high as 480 mW at 1.3 THz. © *2003 American Institute of Physics.* [DOI: 10.1063/1.1560573]

I. INTRODUCTION

Nishizawa predicted the generation of terahertz waves via the resonance of phonons and molecular vibrations.[1,2] Later Nishizawa and Suto[3] realized a semiconductor GaP Raman laser and generated a 12 THz wave with a peak power as high as 3 W by using a GaP Raman oscillator containing a GaAs difference wave-mixing crystal.[4] Loudon made a similar proposal, although he thought that a uniaxial crystal was required.[5] Nishizawa promoted the development of terahertz (THz) wave generation via resonance of phonons and proposed that wavelength-tunable THz waves be used to detect and treat cancers.[6] Under his guidance, Kawase and Ito recently realized frequency-tunable high-power THz wave generation.[7] They obtained 200 mW peak power at 1 THz, by adopting injection seeding in $LiNbO_3$. Note that Yarborough *et al.*[8] reported THz wave generation via $LiNbO_3$. In addition, 29.2, 29.9, and 34.4 μm waves were detected as difference frequency waves in GaP.[9]

We realized Raman lasing oscillation via the parametric mode (polariton mode) in GaP,[3] and pointed out that almost collinear phase matching could be obtained in GaP at pump wavelengths near 1.064 μm.[10] Recently, it was reported that exact collinear phase matching of the difference wave was obtained at wavelengths shorter than 990 nm.[11] This means that exact phase matching should be attainable in GaP at near 1.064 μm with a noncollinear configuration, but with a very small angle between the pump and signal (Stokes) beams.

This article describes efficient continuous frequency tunable THz wave generation from GaP over the frequency range from 0.5 to 3 THz, under precise phase-matching conditions, realized by tuning a very small angle between the pump and signal beam directions.

Recently, we reported stimulated Raman amplification in GaP–AlGaP waveguides, and measured the Raman gain coefficient for the longitudinal optical (LO) phonon mode in GaP to be 12.3×10^{-8} cm W^{-1}.[12,13] This value is the highest Raman gain for various solids and liquids, including $LiNbO_3$ and CS_2, estimated from the spontaneous Raman scattering intensities of these materials. Since difference frequency generation efficiency is related to the parametric Raman gain coefficient, although it is based on transverse optical phonons instead of LO phonons, we can expect efficient THz wave generation in GaP under the exact phase matching condition at 1.064 μm. For this, a convenient YAG laser can be adopted as either the pump or the signal light source.

II. EXPERIMENT

Figure 1 shows a schematic of the experimental setup used for difference frequency generation (DFG) of a THz wave in GaP crystals. The fundamental properties of DFG in GaP, particularly phase matching, were investigated in detail using a low-power YAG laser as the signal source and a β-BaB_2O_4 based optical parametric oscillator (OPO) as the pump source [Fig. 1(a)]. In addition, we attempted to generate a high-power THz wave using a high-power YAG laser instead of a low-power YAG laser [Fig. 1(b)].

The low-power YAG laser (1064 nm) used as the signal source was pumped with a laser diode, delivering about 87 μJ single pulse energy with a 5 mm beam diameter and a pulse duration of 23 ns. The OPO was pumped with the 355 nm line from a *Q*-switched Nd:YAG third harmonic generation laser with a repetition rate of 10 Hz. The energy of the pump beam from the OPO was 4 mJ with a 3 mm beam diameter at a pulse width of 6 ns. The linewidth of the pump beam was 0.2 cm^{-1}. The high-power YAG laser used in the high-power THz wave generation experiment was the same as that used to pump the OPO. Its 1064 nm fundamental

[a]Author to whom correspondence should be addressed; electronic mail: tanabet@material.tohoku.ac.jp

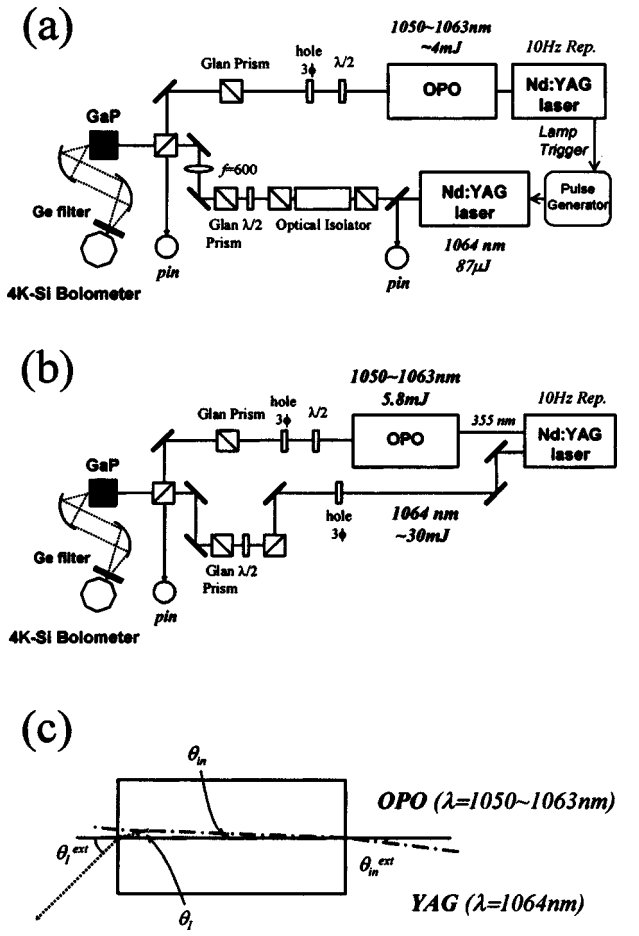

FIG. 1. Schematics of the experimental setup used for THz wave generation in GaP crystals: (a) the low-power YAG laser system, (b) the high-power YAG laser system, and (c) the relationship between the pump and signal beams in a GaP crystal.

output with a pulse width of 11 ns and a linewidth of 0.003 cm^{-1} was used as the signal source after attenuating the pulse energy below 30 mJ.

We used undoped semi-insulating GaP crystals purchased from Sumitomo Metal Mining Co. A GaP crystal was cut into a rectangle 2.6, 5, or 20 mm long in the ⟨110⟩ direction and 3 mm thick in the ⟨001⟩ direction. The input and output faces were polished optically flat and chemically etched. The signal beam delivered from the YAG laser was combined with the pump beam using a cubic polarizer. The incident beams were close to parallel to the ⟨110⟩ crystal direction of GaP. The temporal overlap of the pump and signal beams was adjusted using delay pulse generators. The spatial overlap of the two incident beams was established, so that it interacted with a collinear configuration, and then with a noncollinear configuration with a very small angle of a few tens of minutes between the two beams. The polarization of the pump and signal light was adjusted in the ⟨001⟩ and ⟨110⟩ directions, respectively. The wavelength of the pump beam was varied between $\lambda=1.05$ and 1.063 μm, which corresponded to generated THz wave frequencies between 3.8 and 0.3 THz. The THz wave energy was collected using paraboloid reflectors and detected using a liquid helium-cooled Si bolometer. A Ge plate was used to filter out near-infrared

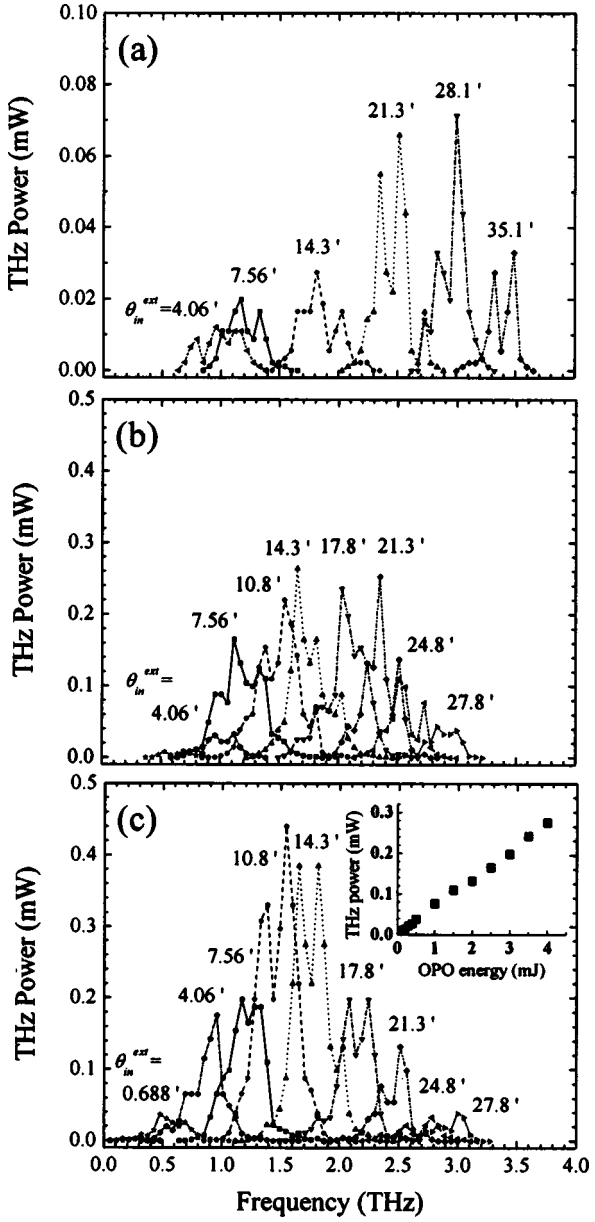

FIG. 2. Frequency dependence of the TH wave output power at various θ_{in}^{ext} in GaP crystals with lengths of: (a) 2.6, (b) 5, and (c) 20 mm. Inset in (c): the THz wave (1 THz) power as a function of the pump beam energy in the 20-mm-long GaP crystal.

(IR) radiation. To measure the high-power THz wave, three Ge plates and a fluorogold/polyethylene filter were used to attenuate the THz power.

III. RESULTS

Figure 2 shows the frequency dependence of the THz wave output power at various θ_{in}^{ext} in GaP crystals with lengths of: (a) 2.6, (b) 5, and (c) 20 mm, where θ_{in}^{ext} is the external angle between the pump and signal beams outside the GaP crystal [Fig. 1(c)]. The internal angle inside the GaP crystal θ_{in} is given by

$$\theta_{in} \approx \frac{\theta_{in}^{ext}}{n_s},$$

where n_s is the refractive index of GaP at 1.064 μm (3.105). No THz wave was detected in any length of GaP crystal when the signal beam paralleled the pump beam (i.e., $\theta_{\text{in}}^{\text{ext}}=0$). Note that in the experiment using the low-power YAG laser, the effective energy/pulse of the signal beam E_{signal}, is determined from the temporal and spatial overlap of the pump beam

$$E_{\text{signal}}=87\ \ \mu\text{J}\times\frac{6\ \ \text{ns}}{23\ \ \text{ns}}\times\left(\frac{3\ \ \text{mm}}{5\ \ \text{mm}}\right)^2=8.2\ \ \mu\text{J}.$$

Thus, the energy/pulse of the signal beam is about 500 times smaller than that of the pump beam (4 mJ). As is shown in Fig. 2(a), THz waves were generated in the 2.6-mm-long GaP over the range from 0.7 to 3.5 THz as $\theta_{\text{in}}^{\text{ext}}$ was varied from 4.06′ to 38.5′. When $\theta_{\text{in}}^{\text{ext}}$ was fixed at 4.06′, the maximum power appeared at 1 THz. The bandwidth for half the maximum power was about 400 GHz when $\theta_{\text{in}}^{\text{ext}}$ was fixed. When $\theta_{\text{in}}^{\text{ext}}$ was increased to $\theta_{\text{in}}^{\text{ext}}=7.56'$, the THz output power increased and the peak frequency shifted to 1.22 THz. Increasing $\theta_{\text{in}}^{\text{ext}}$ shifted the maximum THz output power to higher frequencies, and THz output power increased to 0.07 mW at 3 THz. For $\theta_{\text{in}}^{\text{ext}}=35.1'$, the THz output peak was at 3.44 THz, but the power decreased. Therefore, frequency-tunable THz waves were generated from the 2.6-mm-long GaP crystal over a wide frequency range, from 0.7 to over 3 THz, by angle tuning, with a peak power position as high as 3.1 THz.

As described in Sec. II, a Ge filter was placed in front of the THz- wave detector to prevent the pump and signal beams from affecting the Si bolometer. Therefore, the frequency dependence was found to oscillate, as seen in the spectra in Fig. 2; this was derived from THz wave resonance with the Ge filter.

As is seen from Fig. 2(b), in the 5-mm-long GaP crystal, a THz wave was generated when $\theta_{\text{in}}^{\text{ext}}$ exceeded 0.688′. An increase in $\theta_{\text{in}}^{\text{ext}}$ caused a shift in the THz wave maximum power position to a higher frequency, and an increase in THz output power. This is very similar to what occurred in the 2.6-mm-long GaP crystal, except that the maximum THz wave output increased to about 0.25 mW, and it appeared at lower frequencies (1.75–2.37 THz) at $\theta_{\text{in}}^{\text{ext}}\approx 14.3'-21.3'$.

Figure 2(c) shows that the THz wave output in a 20-mm-long GaP crystal ranged from 0.5 to 2.95 THz, which is a lower frequency range than for the 2.6- and 5-mm-long crystals. The output power was further increased. The maximum THz wave output power was 0.44 mW, and appeared at an even lower frequency, 1.44 THz. The THz wave output power at 1 THz was proportional to the pump beam energy, as shown in the inset of Fig. 2(c).

The peak frequency position of the THz wave output power for each $\theta_{\text{in}}^{\text{ext}}$ observed in Fig. 2 is plotted as a function of $\theta_{\text{in}}^{\text{ext}}$ in Fig. 3, which shows that the THz wave frequency increased nearly linearly with the angle between the pump and signal beams, irrespective of the crystal length. The slope of the curve is 11.6′/THz=3.36 mrad/THz, at around 1.5 THz. This means that a continuously frequency tunable THz wave from 0.6 to 3.5 THz can be generated in GaP crystals by continuously adjusting the angle between the pump and signal beams over a range of less than 1°.

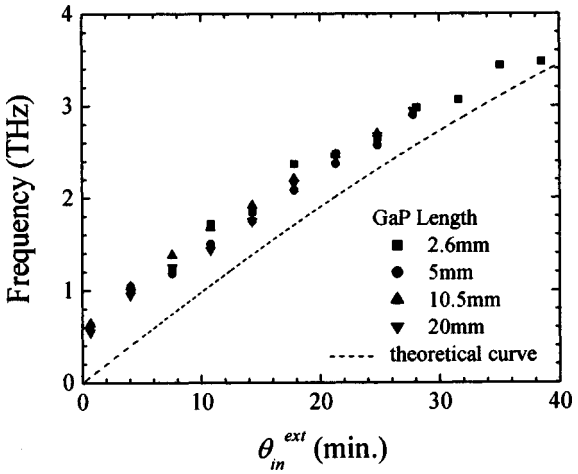

FIG. 3. Dependence of $\theta_{\text{in}}^{\text{ext}}$ on the peak frequency position of the THz wave output power.

The THz wave output power at various THz frequencies is plotted against the GaP crystal length in Fig. 4. This clearly shows that the power increased steeply with increasing crystal length from 2.6 to 5 mm. The THz power is likely proportional to the square of the crystal length l (l^2 dependence is indicated by the dashed line in Fig. 4). From 5 to 20 mm, the power increased further in the range 1.22–1.78 THz, but not as much as expected from l^2 dependence. This implies that the coherence length l_{coh}, is well over 5 mm, but is less than 20 mm. In contrast, the THz wave output power at frequencies of 2.2–2.63 THz decreased in the 20 mm crystal. This may be due to the absorption of higher frequency THz waves in GaP crystal, as discussed below.

The angle between the directions of the pump beam and the THz wave leaving the GaP crystal end face (θ_I^{ext}) is plotted as a function of $\theta_{\text{in}}^{\text{ext}}$ for different crystal lengths in Fig. 5. In this measurement, the THz wave was detected directly by placing a Si bolometer in front of the GaP crystal output face, without focusing the wave with paraboloid reflectors. For every length of GaP crystal, θ_I^{ext} tended to increase with the incident beam angle $\theta_{\text{in}}^{\text{ext}}$. Simultaneously, the

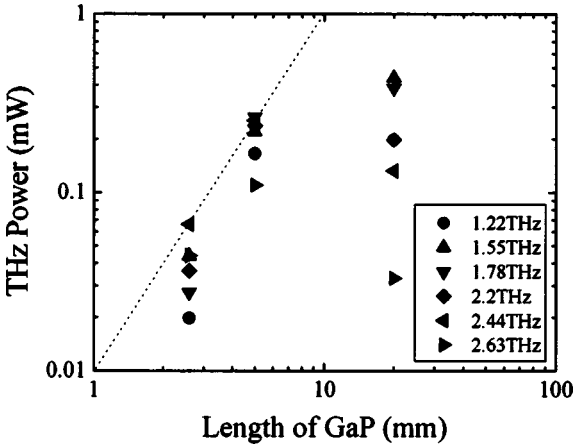

FIG. 4. THz wave output power at various THz frequencies (1.22–2.63 THz) plotted against GaP crystal length. The dashed line indicates l^2 dependence.

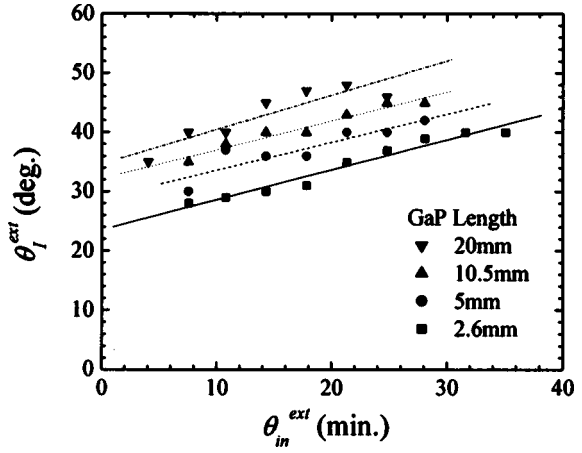

FIG. 5. The angle between the pump beam direction and the direction of the THz wave propagating from the GaP crystal end face (θ_I^{ext}) for various GaP crystal lengths.

longer the GaP crystal, the larger θ_I^{ext}. The THz wave generated in a 20-mm-long GaP crystal leaves the GaP crystal output-face at 35°–45° to the normal. This contrasts with the frequency $-\theta_{\text{in}}^{\text{ext}}$ relation, which is nearly independent of the crystal length (see Fig. 3), and there is a considerable deviation from the expectation that θ_I^{ext} should be almost constant (58.1°) under phase-matching conditions. This is discussed below.

Finally, Fig. 6 shows the THz wave power generated as a function of the signal beam energy measured using the high-power YAG laser instead of the low-power YAG laser. In this experiment, the signal beam energy/pulse was effectively increased to 1.6×10^3 times that using the low-power YAG laser. The wavelength of the pump beam from the OPO was 1.0592 μm with the energy/pulse fixed at 5.8 mJ. A THz wave of 1.3 THz was generated at $\theta_{\text{in}}^{\text{ext}}=8.68'$ in the 20-mm-long GaP crystal. It can be seen that the THz wave power was nearly proportional to the YAG energy/pulse. When the signal energy/pulse of the YAG laser was 26 mJ, the maximum THz power achieved was 480 mW.

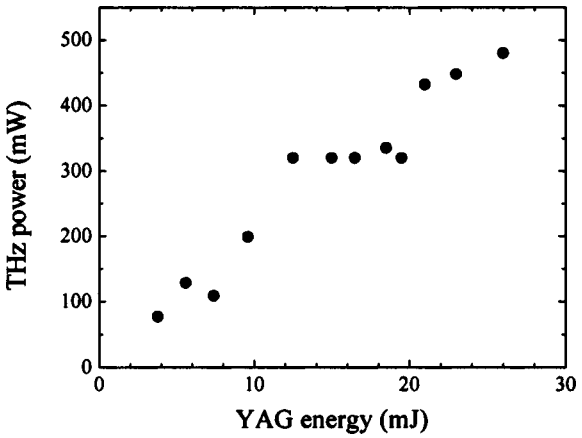

FIG. 6. Generated THz wave power as a function of the signal beam energy/pulse in the 20-mm-long GaP crystal. The pump beam energy/pulse was 5.8 mJ.

IV. DISCUSSION

We discuss the phase-matching properties. If the deviation from the phase-matching condition for the collinear interaction is so small that the angle inside the crystal between the pump and signal (Stokes) beams for noncollinear interaction satisfies $\theta_{\text{in}}\ll1$, then, the wave vectors of the pump, signal, and THz waves (idler wave), $\mathbf{k}_L$, $\mathbf{k}_S$, and $\mathbf{q}$, respectively, must satisfy the following equation, as derived from the geometric relation of the vectors illustrated in Fig. 1(c):[14]

$$\frac{\Delta q}{q}=2\left(\frac{\mathbf{k}_L\cdot\mathbf{k}_S}{\mathbf{q}^2}\right)\cdot\sin^2\left(\frac{\theta_{\text{in}}}{2}\right)\approx\frac{1}{2}\left(\frac{n_Ln_S}{n_I^2}\right)\cdot\left(\frac{\nu_L\nu_S}{\nu^2}\right)\cdot\theta_{\text{in}}^2, \tag{1}$$

where, Δq is the deviation of q in the collinear configuration from the exact collinear phase matching value, and ν_L, ν_S, and υ are the frequencies of the pump, signal, and THz waves, respectively.

From this equation, the angle for noncollinear phase matching, θ_{in}, changes almost linearly with the THz frequency, as given by

$$\frac{\theta_{\text{in}}}{\nu}=\sqrt{\frac{2\left(\frac{\Delta q}{q}\right)\cdot\left(\frac{n_I^2}{n_Ln_S}\right)}{\nu_L\nu_S}}. \tag{2}$$

θ_{in}/ν is nearly constant, because we can assume that $\Delta q/q$ changes only slightly with the frequency ν in the THz frequency region from 0.5 to 3 THz. The result given in Fig. 3 shows that the slope $d\theta_{\text{in}}^{\text{ext}}/d\nu$ is about 3.36 mrad/THz at around 1.5 THz, where $\theta_{\text{in}}^{\text{ext}}$ is the angle between the pump and signal beams outside the crystal, given by $\theta_{\text{in}}^{\text{ext}}\approx3.105\theta_{\text{in}}$. Therefore, we obtain $\theta_{\text{in}}/\nu=1.08$ mrad/THz, at around 1.5 THz. From this value, the relative deviation from phase matching under the collinear condition ($\Delta q/q$) is calculated to be 0.040 (4.0%).

This result can be confirmed in another way. For the collinear interaction, the difference between the pump and signal wave numbers can be described by the following equations:

$$\mathbf{k}_L-\mathbf{k}_S=\mathbf{k}=\frac{\mathbf{n}_{\text{eff}}\cdot2\pi\nu}{c}, \tag{3}$$

$$n_{\text{eff}}=n_S+\boldsymbol{\nu}_L\cdot\frac{\delta n}{\delta\nu}, \tag{4}$$

where $\delta n/\delta\nu$, the frequency dispersion of the refractive index, is 4.66×10^{-4}/THz,[15] and the refractive index for the signal light is $n_s=3.104\,84$. Then, $n_{\text{eff}}=3.236\,90$ is obtained for $\lambda_S=1.064$ μm. Moreover, the polariton dispersion relationship for the THz wave is given by the following equation:

$$\left(\frac{cq}{2\pi\nu}\right)^2=n_I^2=\frac{(\varepsilon_S\nu_0^2-\varepsilon_\infty\nu^2)}{(\nu_0^2-\nu^2)}, \tag{5}$$

with $\varepsilon_S = 11.15$, $\varepsilon_\infty = 9.20$, and $\nu_0 = 11.01$ THz for GaP.[16] From this relation, the refractive index in the THz region, $n_I = 3.3445$, is obtained for $\nu = 1.5$ THz. Therefore, the wave number mismatch $(\Delta q/q) = (n_I - n_{\text{eff}})/n_I = 0.0323$ is obtained at 1.5 THz. This result is approximately coincident with that obtained from Fig. 3.

The angle of the propagation direction of the THz wave inside the crystal, θ_I, is given as follows, from the geometric relationship illustrated in Fig. 1(c):

$$\sin(\theta_I - \theta_{\text{in}}) = \left(\frac{k_S}{q}\right) \sin\ \theta_{in}, \quad \text{with} \quad \theta_I \gg \theta_{\text{in}},$$

then, we obtain

$$\sin\ \theta_I \approx \sqrt{\left(\frac{2\Delta q}{q}\right) \cdot \left(\frac{\nu_S}{\nu_L}\right) \cdot \left(\frac{n_S}{n_L}\right)} \approx \sqrt{\frac{2\Delta q}{q}}. \tag{6}$$

That is, θ_I is simply related to the relative deviation from phase matching in the collinear interaction, $\Delta q/q$. It should be nearly constant with changes in ν, except for the slight change due to the dispersion given in Eq. (5). From $\Delta q/q \approx 0.032$, θ_I is calculated to be $\theta_I = 14.7°$ at around 1.5 THz. Then, the direction angle of the THz wave outside the crystal should become $\theta_I^{\text{ext}} = 58.1°$.

The experimentally observed θ_I^{ext}, however, was considerably smaller than this value. Moreover, θ_I^{ext} increased with $\theta_{\text{in}}^{\text{ext}}$, and with increasing crystal length, as shown in Fig. 5. The observed θ_I^{ext} was in the range 28°–48°, which corresponds to θ_I in the range 8.1°–12.8°.

As a possible reason for this discrepancy, we postulate that the direction determined by Eq. (5) is that of the nonlinear polarization, *P*, while the actual propagation directions of the electromagnetic fields *E* and *H* of the THz wave are closer to the axes of the pump and signal beams, because their energy distributions are not those of pure plane waves, but are considerably larger near their axes. When the crystal length is much smaller than the coherence length, any direction around the angle determined as the direction of the wave vector of nonlinear polarization *P* becomes a possible propagation direction, so the actual propagation direction may become closer to the axes of the pump and signal beams. This contrasts with the definite propagation directions of the pump and signal waves. As the crystal length increases and approaches the coherence length, as with the 20-mm-long crystal, the propagation direction becomes closer to that determined from nonlinear polarization, *P*.

A similar explanation may hold for the increase in θ_I with increasing θ_{in} (increasing THz frequency ν). The increase in ν may reduce the accuracy of noncollinear phase matching, due to the increase in the absorption coefficient of the THz wave arising from lattice absorption. As a result, the coherence length should be reduced. This is equivalent to increasing the crystal length relative to the coherence length, so that the THz wave direction approaches that determined from *P*.

As seen in Fig. 2(a), the peak THz power appeared at 3 THz for the 2.6-mm-long crystal, but the peak frequency decreased with increasing crystal length, falling to 1.5 THz for the 20-mm-long crystal. This tendency is also thought to be an effect of increased THz wave absorption at higher THz frequencies.

As a result of phase matching via angle tuning, the coherence length l_{coh}, for difference wave generation increases. If l_{coh} is sufficiently larger than the crystal length, *l*, the THz power is expected to be proportional to l^2.[17] In this experiment, although the 20-mm-long sample gave the highest THz intensity, it did not increase as much as expected from l^2 dependence, as shown in Fig. 4. Consequently, we postulate that the coherence length at around 1.5 THz after angle tuning is roughly in the range from 10 to 20 mm. In addition, Fig. 4 shows that at larger θ_{in} (larger ν), the intensities for the 20-mm-long crystal were smaller than those for the 5-mm-long crystal. This implies that stronger lattice absorption at larger ν decreases both the intensity and coherence length of the THz wave.

Next, we discuss the maximum THz power. In the experiment using the low-power YAG laser as the signal source, the pump light from the OPO laser had an energy of 4 mJ, a pulse width of 6 ns, and a beam diameter of 3 mm (peak intensity 9.5 MW/cm^2), while the signal light from the low-power YAG laser had an effective energy/pulse of 8.2 μJ, with the same pulse width and diameter. Under these conditions, we obtained a maximum peak power of 0.4 mW at 1.5 THz.

With difference wave mixing, the THz wave output power is expected to be proportional to the product of the pump and signal power, as long as we neglect the amplifying effect of the signal and THz waves. Using a high-power YAG laser, we realized a pulse peak power of 480 mW at 1.3 THz, under the following conditions: OPO: 5.8 mJ (14 MW/cm^2), YAG: 26 mJ (33 MW/cm^2), as shown in Fig. 6. The THz output power was nearly the same as that extrapolated from the result using the low- power YAG laser as the signal source.

Note that presently the only practical parametric generator is based on $LiNbO_3$. With a conventional $LiNbO_3$ THz parametric generator, the THz output power is on the order of milliWatts. Recently, however, the maximum THz output power has been increased to 200 mW, achieving a very narrow linewidth, by introducing the injection-seeding technique.[7] In this experiment, the THz output power from GaP exceeded the power from $LiNbO_3$, although injection seeding was not adopted. Our result for THz wave generation coincides with our recent result showing that the Raman gain coefficient in GaP is higher than that in $LiNbO_3$.

V. CONCLUSION

A frequency-tunable terahertz wave was generated from GaP crystals as a difference wave using an optical parametric oscillator (1.050–1.063 μm) as the pump source and a YAG laser (1.064 μm) as the signal source. Noncollinear phase matching with a very small angle between the pump and signal light beam directions, θ_{in}, of less than 35 min was required. The THz frequency changed almost linearly with θ_{in}. As a result, tunable THz waves with frequencies from

0.5 to 3 THz were obtained, with a less than tenfold change in the output power level. The pulsed peak power of the THz wave was as high as 480 mW at 1.3 THz.

GaP crystals are a promising candidate as a practical THz wave source with high output power, possibly at the 1 W level, and wide frequency tunability.

ACKNOWLEDGMENT

This work was supported by a Grant-in-Aid for Creative Scientific Research (No. 13GS0002) from the Japan Society for the Promotion of Science.

[1] J. Nishizawa, Densi Kagaku **13**, 17 (1963) (in Japanese).
[2] J. Nishizawa, Denshi Gijutu **7**, 101 (1965) (in Japanese).
[3] J. Nishizawa and K. Suto, J. Appl. Phys. **51**, 2429 (1980).
[4] K. Suto and J. Nishizawa, IEEE J. Quantum Electron. **QE-19**, 1251 (1983).
[5] R. R. Loudon, Proc. Phys. Soc. London **82**, 393 (1963).
[6] J. Nishizawa, J. Acoust. Soc. Jpn. **57**, 163 (2001).
[7] K. Kawase, H. Minamide, K. Imai, J. Shikata, and H. Ito, Appl. Phys. Lett. **80**, 195 (2002).
[8] J. M. Yarborough, S. S. Sussman, H. E. Purhoff, R. H. Pantell, and B. C. Johnson, Appl. Phys. Lett. **15**, 102 (1969).
[9] F. De Martini, in *Light Scattering in Solids*, edited by M. Balkanski (Flammarsion Sciences, Paris, 1971), pp. 201–220.
[10] J. Nishizawa and K. Suto, in *Infrared and Millmeter Waves 7*, edited by K. J. Button (Academic, New York, 1983), pp. 301–320.
[11] T. Taniuchi, J. Shikata, and H. Ito, Proceedings of the 8th IEEE International Conference on Terahertz Electronics, , 2000, Vol. P-8, pp. 225–228.
[12] T. Saito, K. Suto, T. Kimura, and J. Nishizawa, J. Appl. Phys. **87**, 3399 (1999).
[13] K. Suto, T. Saito, T. Kimura, J. Nishizawa, and T. Tanabe, J. Lightwave Technol. **20**, 705 (2002).
[14] C. H. Henry and J. J. Hopfield, Phys. Rev. Lett. **15**, 964 (1965).
[15] W. L. Bond, J. Appl. Phys. **36**, 1674 (1965).
[16] A. Mooradian and G. B. Wright, Solid State Commun. **4**, 431 (1966).
[17] T. Yajima and K. Inoue, IEEE J. Quantum Electron. **QE-5**, 140 (1969).